Approaches to stratified sampling and variance reduction in outdoor sound propagation calculations

D. Keith WILSON[1]; Carl R. HART[2]; Michelle E. SWEARINGEN[3]; Chris L. PETTIT[4]

[1,2]U.S. Army Engineer Research and Development Center, Hanover, NH, USA

[3]U.S. Army Engineer Research and Development Center, Champaign, IL, USA

[4]United States Naval Academy, Annapolis, MD, USA

ABSTRACT
To facilitate efficient predictions of outdoor sound propagation, meteorological and refractive conditions are often partitioned into statistical strata (classes). Average predictions are then made by weighting individual predictions from each stratum. Some examples are Marsh's scheme based on Pasquill stability classes, the Harmonoise scheme based on a log-linear parameterization of the effective sound-speed profile, and various schemes utilizing Monin-Obukhov similarity theory parameters. The success of stratified sampling depends on whether useful classes can be chosen, in the sense of efficiently capturing the diversity of propagation conditions, while reducing the variance within the classes. The overall reduction in error variance can be quantified using equations known from statistics. In this paper, we adopt such an approach to analyzing the performance of several sampling strategies, and illustrate situations for which stratified sampling provides improved variance reduction.

Keywords: Numerical Modeling, Statistical Methods
I-INCE Classification of Subjects Number(s): 24.6, 77

1. INTRODUCTION

Many schemes have been proposed for categorizing atmospheric and ground conditions according to their impact on outdoor sound propagation. At the simplest, ground categories may specify whether the surface is acoustically hard (such as asphalt or frozen ground) or soft (such loose soil or snow). Atmospheric categories may, for example, specify whether refraction is strong upward, weak upward, intermediate, weak downward, or strong downward. The purpose for formulating such classes of conditions is usually to create efficient, heuristic schemes for predicting sound levels. For example, a sound-level prediction might be made for each category based on experimental data or a more intensive numerical method (such as the parabolic equation), and then this prediction would be applied to all other ground and atmospheric conditions falling into that category.

Some of the most widely used schemes for refractive categories have been based on classes or theories originally appearing in the meteorological literature. For example, Marsh [1] employed Pasquill's stability classes [2] for turbulent diffusion modeling (based on wind speed and solar radiation) to partition sound propagation conditions into six refractive classes. Zouboff et al. [3] also formulated refractive classes based on Pasquill. Raspet and Wolf [4] partitioned calculations by wind speed and direction intervals. Heimann and Salomons [5] approximated Monin-Obukhov similarity theory (MOST) profiles with log-linear profiles and then formulated a scheme with 25 refractive classes based on ranges of the log-linear profile parameters.

[1]d.keith.wilson@usace.army.mil
[2]carl.r.hart@erdc.dren.mil
[3]michelle.e.swearingen@usace.army.mil
[4]pettitcl@usna.edu

The refraction categories or other types of propagation classes can conceivably be employed in at least a couple different ways. First is the classical problem of variance reduction — we wish to make an accurate prediction from as few samples (numerical predictions or experimental observations) as possible. If the classes are chosen in a manner that successfully captures most of the variability in the process, we can accurately estimate the quantity of interest in each class with relatively few samples.

The other method of employment is perhaps more common in outdoor sound propagation modeling. This involves (1) running a relatively expensive computational method (the parabolic equation, for example) one or more times to predict a representative sound intensity for each class, (2) determining the probabilities for each class at a particular site of interest, and (3) determining an estimate for the overall mean as a weighted sum of the predictions for the individual classes. Note that this approach involves generating the predictions for each class just once; the predictions are then assumed to be applicable to any site.

Propagation classes might also be motivated from the perspective of *parsimony* in outdoor sound propagation predictions. Although the fundamental physics underlying sound propagation are well understood, modeling capabilities are typically inadequate to capture all of the intricacies. Thus, simpler and less computationally expensive (lower order) modeling approaches may be more consistent with the actual predictability of outdoor sound propagation.

This paper endeavors to examine the problem of categorizing sound propagation conditions from a broader, more fundamental perspective than is normally done. The goal is to explicitly examine the statistical benefits, qualitative and quantitative, of such schemes, and to help guide future research towards more optimally formulating the categories. We point out that the fundamental problem is hardly novel in the realm of statistics: it is a particular example of *stratified sampling*. Nonetheless, from a research perspective outdoor sound propagation provides a very interesting application of stratified sampling, as it invokes many challenging issues related to modeling and quantifying uncertainties in a complex, highly multidimensional system.

The first section of this paper overviews the general analytical framework of stratified sampling and variance reduction. The second section describes an application to sound refraction outdoors.

2. FORMULATION OF THE SAMPLING PROBLEM

2.1 Parameters and Distributions

For present purposes, we view environmental parameters impacting the sound propagation as random variables. Such parameters may include the porosity and static flow resistivity of the ground, landcover properties such as vegetation and man-made structures, and meteorological quantities such as the friction velocity and surface heat flux. These parameters vary randomly in time, on scales from minutes to seasonal, and in space, on scales from meters to globally (*aleatory* uncertainties). We may also be compelled to represent the environmental parameters as random variables because our knowledge is limited (*epistemic* uncertainties) [6].

Sound propagation predictions are made for a particular sample (or samples) of the environmental parameters, the sample formally being drawn from an assumed joint probability density function (pdf) of the parameters. For example, if the wind direction is variable, we could specify a distribution for it, randomly sample from the distribution, and then perform a propagation calculation for each sample direction. Quantities of interest, such as the mean and variance of the squared sound pressure, can then be estimated from the ensemble of predictions.

Mathematically, we write the probability that a continuous random variable Θ will take on a value in the interval $[\theta, \theta + \Delta\theta]$ as

$$\Pr[\theta \leq \Theta \leq \theta + \Delta\theta] = \int_{\theta}^{\theta+\Delta\theta} g(\xi)\, d\xi, \tag{1}$$

where $g_\Theta(\theta)$ is the single-variate pdf. The cumulative distribution function (cdf), $G_\Theta(\theta)$, is the probability that Θ will take on a value less than or equal to θ, namely $G_\Theta(\theta) = \Pr[\Theta \leq \theta] = \int_{-\infty}^{\theta} g_\Theta(\xi)\, d\xi$. By differentiating the integral, we have $g_\Theta(\theta) = dG_\Theta(\theta)/d\theta$.

The uniform, beta, normal (Gaussian), log-normal, exponential, and Rayleigh distributions are particularly useful for continuous random variables, and often appear in problems involving wave propagation and scattering. The type of distribution and parameter values depend greatly on the application. The best practice is generally to employ the simplest distribution consistent with the known constraints and available observations.

The definitions for a single variable can be readily extended to a set of M random variables grouped as a vector, $\mathbf{\Theta} = [\Theta_1, \Theta_2, \ldots, \Theta_M]$. In our case, this set represents all of the environmental parameters which we wish to model as being random or uncertain. The joint pdf of these variables, $g_{\mathbf{\Theta}}$, is defined such that

$$\Pr[\mathbf{\Theta} \in \Omega'] = \int_{\Omega'} g_{\mathbf{\Theta}}(\theta_1, \ldots, \theta_M)\, d\theta_1 \ldots d\theta_M, \tag{2}$$

where Ω' is a subdomain within the overall domain Ω upon which $\mathbf{\Theta}$ is defined ($\Omega' \in \Omega$). The cdf is defined as $G(\theta_1, \ldots, \theta_M) = \Pr[\Theta_1 \leq \theta_1 \cdots \Theta_M \leq \theta_M]$. If the variables in $\mathbf{\Theta}$ are independent, one has $g_{\mathbf{\Theta}}(\theta_1, \ldots, \theta_M) = g_{\Theta_1}(\theta_1) \cdots g_{\Theta_M}(\theta_M)$.

The expected value of a function $I(\boldsymbol{\theta})$ can be calculated from the integral [7, 8]

$$\langle I \rangle = \int_{\Omega} I(\boldsymbol{\theta}) g_{\mathbf{\Theta}}(\boldsymbol{\theta})\, d\boldsymbol{\theta}. \tag{3}$$

The integrand $I(\boldsymbol{\theta})$ may represent the squared magnitude of the sound pressure (intensity), excess attenuation, sound level, or other quantity of interest. It is convenient to transform independent variables to uniform distributions in the range $[0, 1]$. This can be done by setting $\psi_m(\theta_m) = G_{\Theta_m}(\theta_m)$, where $G_{\Theta_m}(\theta_m)$ is the cdf for the mth parameter ($m = 1, \ldots, M$), resulting in

$$\langle I \rangle = \int_{U} I(\boldsymbol{\theta}(\boldsymbol{\psi}))\, d\boldsymbol{\psi}. \tag{4}$$

Here U indicates the M-dimensional unit volume. The values of the variables are then determined from the inverse cdfs: $\theta_m = G^{-1}_{\Theta_m}(\psi_m)$.

2.2 Ordinary Monte Carlo Sampling

Many science and engineering problems involve a large number of random parameters, thus making Eq. (3) and its variants highly multidimensional [9, 10]. A conventional numerical approach to integrating Eq. (3) would involve discretizing the integral into a finite number of intervals along each of the M variable axes. However, the number of evaluations of the integrand then increases geometrically according the number of dimensions in the integral (random variables or parameters). Stochastic techniques are particularly valuable in such situations, as all of the parameters can be sampled simultaneously [9, 11]. The basic process involves generating N samples of the parameter set $\mathbf{\Theta}$ ($\mathbf{\Theta}_n$, $n = 1, 2, \ldots, N$). The function $I(\mathbf{\Theta})$ is evaluated for each of these samples. The average of these N evaluations, $\hat{I}$, then gives an estimate for the mean $\langle I \rangle$:

$$\hat{I} = \frac{1}{N} \sum_{n=1}^{N} I(\mathbf{\Theta}_n). \tag{5}$$

The variance of the estimate is given by

$$\sigma^2_{\hat{I}} = \left\langle \left[\hat{I} - \langle I \rangle\right]^2 \right\rangle = \frac{1}{N^2} \left\langle \left\{ \sum_{n=1}^{N} [I(\mathbf{\Theta}_n) - \langle I \rangle] \right\}^2 \right\rangle. \tag{6}$$

A general result for $\sigma^2_{\hat{I}}$, which does not assume $\hat{I}$ is an unbiased estimator for $\langle I \rangle$, is [6]

$$\sigma^2_{\hat{I}} = \frac{1}{N^2} \sum_{n=1}^{N} \sigma^2(\mathbf{\Theta}_n) + \frac{1}{N^2} \left[\sum_{n=1}^{N} b(\mathbf{\Theta}_n) \right]^2, \tag{7}$$

where

$$\sigma^2(\mathbf{\Theta}) = \left\langle [I(\mathbf{\Theta}) - \langle I(\mathbf{\Theta}) \rangle]^2 \right\rangle \tag{8}$$

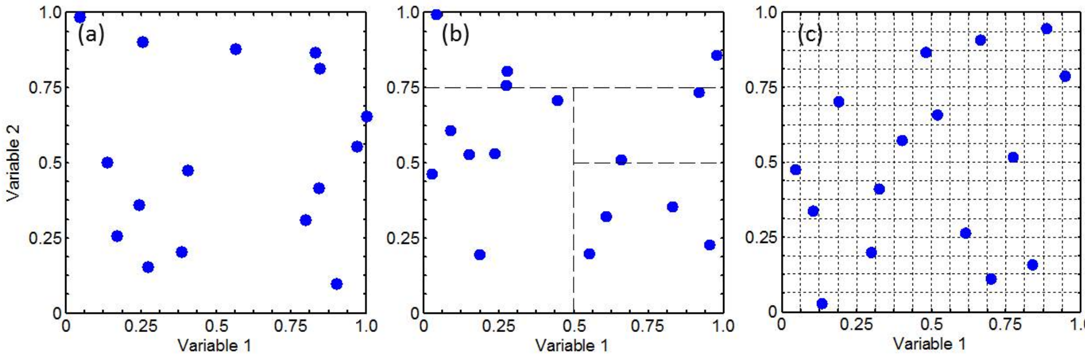

Figure 1: Comparison of several strategies to obtain 16 samples of two independent, uniform random variables. (a) Ordinary Monte Carlo sampling (MCS). (b) Stratified sampling with four unequal strata. (c) Ordinary Latin hypercube sampling (LHS) with an iterative maximin criterion.

and

$$b(\mathbf{\Theta}) = \langle I(\mathbf{\Theta}) \rangle - \langle I \rangle \tag{9}$$

are the variance and bias of the integrand as a function of $\mathbf{\Theta}$, respectively.

The preceding discussion describes *ordinary Monte Carlo sampling*, or MCS. Typically, the $\mathbf{\Theta}_n$ are drawn independently from the joint pdf. Then each evaluation of the integrand is an equally likely value, and $\hat{I}$ is thus an unbiased estimate for $\langle I \rangle$, which converges to the correct value as N increases. The variance of the estimate then reduces to simply $\sigma_{\hat{I}}^2 = \sigma^2/N$, in which $\sigma^2 = \left\langle [I - \langle I \rangle]^2 \right\rangle$.

The main procedure for incorporating turbulent scattering into sound propagation calculations is to generate random realizations of turbulence fields [12, 13]. The sound intensity is then calculated for each realization, and the calculations averaged. This procedure exemplifies Monte Carlo sampling; the phase of each Fourier mode can be viewed as the sample of a random variable with uniform distribution between 0 and 2π. Since the random scattering produces a standard deviation of about 6 dB, the sound-level estimate has root-mean-square (rms) error of (6 dB)$/\sqrt{N}$. But it has not been as widely appreciated that, when such random realizations of the turbulence are generated, the additional computational cost of simultaneously sampling other random variables, such as those associated with uncertainties in the ground properties and atmospheric parameters, is negligible.

Ordinary MCS is illustrated in Fig. 1(a), for a case involving 16 samples of two independent random variables, each distributed uniformly over the range $[0, 1]$.

2.3 Stratified and Latin Hypercube Sampling

A drawback of MCS is that it tends to randomly undersample certain parts of the input parameter space, while oversampling others. *Stratified sampling* is commonly employed to ensure that important regions of the parameter space are adequately sampled. The parameter space is partitioned into strata, and then each stratum is sampled independently. The overall statistics are determined by appropriately weighting statistics as calculated from the individual strata. The strata should be mutually exclusive and exhaustive.

Let us consider K strata, designated Ω_k (where $\Omega_k \in \Omega$ and $k = 1, \ldots, K$), with p_k being the probability of the parameters occurring within stratum k. Within each stratum, N_k random samples of $\mathbf{\Theta}$ are drawn (e.g., using ordinary MCS), which we designate $\mathbf{\Theta}_{k,n}$ ($n = 1, \ldots, N_k$, where $\sum_k N_k = N$ is the total number of samples). The estimate for the mean within stratum k is

$$\hat{I}_k = \frac{1}{N_k} \sum_{n=1}^{N_k} I(\mathbf{\Theta}_{k,n}). \tag{10}$$

The overall estimate for $\langle I \rangle$ is then determined from the estimated means of the strata as

$$\hat{I} = \sum_{k=1}^{K} p_k \hat{I}_k. \tag{11}$$

In most applications of stratified sampling, *proportionate* sampling is used, meaning that N_k is set to $p_k N$. Figure 1(b) illustrates this approach. Here, the parameter space for two variables has been partitioned into four strata ($K = 4$). As drawn in the figure, the strata have probability $p_1 = 1/4$, $p_2 = 1/8$, $p_3 = 1/4$, and $p_4 = 3/8$. Hence, for a total of $N = 16$ samples, $N_1 = 4$, $N_2 = 2$, $N_3 = 4$, and $N_4 = 6$.

The variance for stratified sampling is derived in Ref. [6] as

$$\sigma_{\hat{I}}^2 = \sum_{k=1}^{K} p_k^2 \sigma_{\hat{I}_k}^2 + \left[\sum_{k=1}^{K} p_k b_{\hat{I}_k} \right]^2, \tag{12}$$

where

$$\sigma_{\hat{I}_k}^2 = \left\langle \left[\hat{I}_k - \langle \hat{I}_k \rangle \right]^2 \right\rangle = \frac{1}{N_k^2} \sum_{n=1}^{N_k} \sigma^2(\mathbf{\Theta}_{k,n}) + \frac{1}{N_k^2} \left[\sum_{n=1}^{N_k} b(\mathbf{\Theta}_{k,n}) \right]^2 \tag{13}$$

and

$$b_{\hat{I}_k} = \langle \hat{I}_k \rangle - \langle I_k \rangle \tag{14}$$

are the variance and bias, respectively, for sampling of the kth stratum. The overall bias of the estimator is

$$b_{\hat{I}} = \sum_{k=1}^{K} p_k b_{\hat{I}_k} = \sum_{k=1}^{K} p_k \langle \hat{I}_k \rangle - \langle I \rangle, \tag{15}$$

in which $\langle I \rangle = \sum_k p_k \langle I_k \rangle$.

When ordinary MCS is applied *within* each stratum, the samples are unbiased ($b(\mathbf{\Theta}_{k,n}) = 0$) and the $\sigma^2(\mathbf{\Theta}_{k,n})$ all take on the same value, namely σ_k^2. Then $\sigma_{\hat{I}_k}^2 = \sigma_k^2 / N_k$ and we have simply

$$\sigma_{\hat{I}}^2 = \sum_{k=1}^{K} \frac{p_k^2 \sigma_k^2}{N_k} + \left[\sum_{k=1}^{K} p_k b_{\hat{I}_k} \right]^2, \tag{16}$$

If the strata are sampled proportionately and the $\hat{I}_k$ are unbiased estimates of $\langle I_k \rangle$, we find that $\sigma_{\hat{I}}^2 = (\sum_k N_k \sigma_k^2)/N^2$, where is the variance within the kth stratum. Should the σ_k^2 happen to all equal the same value, σ^2, this result reduces to ordinary MCS applied throughout the domain.

Latin hypercube sampling (LHS) is a general and relatively simple approach to stratified sampling which, unlike most stratified sampling procedures, can be readily applied to situations involving many variables [14]. The range for each of the M variables is first partitioned into N equal-probability intervals. The resulting grid has $K = N^M$ strata. A single sample is randomly drawn from each of the N intervals for each variable. Note that only a subset of the strata are actually sampled; in fact, the probability of any given stratum being sampled is N^{1-M}, which becomes very small when M is large. LHS is illustrated in Fig. 1(c). Like ordinary MCS, the LHS estimate $\hat{I}$ for $\langle I \rangle$ can be calculated from Eq. (5). The estimate is unbiased, since the strata are sampled with equal likelihood. Unlike MCS, however, the samples are not drawn independently.

Let us consider an illustrative example of the benefits of stratified sampling. The example involves two independent random variables. The ranges for each variable are partitioned into four equal-probability intervals, resulting in a matrix with $4 \times 4 = 16$ strata. Three cases are considered here which involve altering the strength of the variations of the means of the strata, $\langle I_k \rangle$. These three cases are shown in Fig. 2. Specifically, Fig. 2(a) is the "strong variation" case, in which the standard deviation of the stratum means is about 4.1. Fig. 2(b) is the "moderate variation" case, with standard deviation of 1.2, and 2(c) is the "weak variation" case, with standard deviation of 0.41. In all cases, the predictions within each stratum are assumed to be

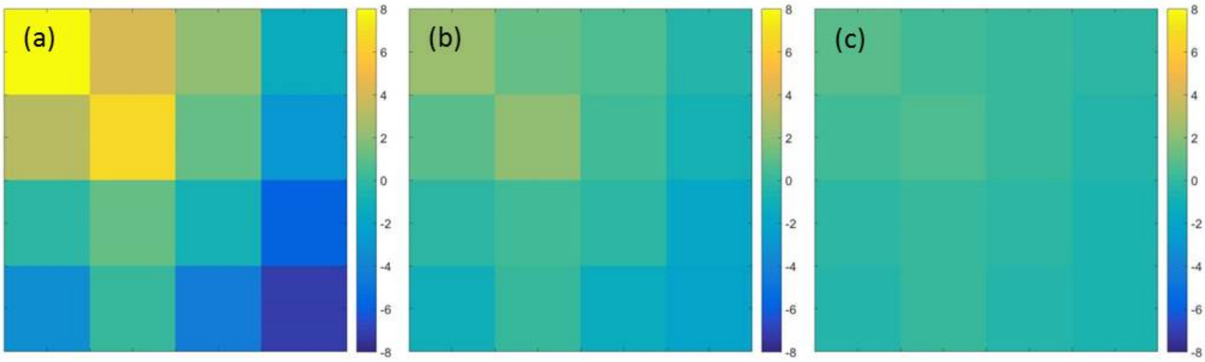

Figure 2: Example problem for stratified sampling of two independent random variables. The ranges for each variable are partitioned into four equal-probability intervals, resulting in 16 strata. The color scale, which indicates the mean for each stratum, ranges from -8 to 8. Three cases involving differing levels of variations of the mean are shown: (a) "strong", (b) "moderate", and (c) "weak". These cases are described in more detail in the text.

unbiased (that is, $\langle \hat{I}_k \rangle = \langle I_k \rangle$), and the variances of the strata, $\sigma^2_{\hat{I}_k} =$, are all set to 1. Hence the strong variation case is dominated by variations between size classes, whereas the weak variation case is dominated by variations within size classes. We would expect stratified sampling to provide the best benefits in the former situation. Note that this example is highly idealized; in a more realistic example, the mean and standard deviation would both vary continuously over the parameter space.

Figure 3 compares the rms error in estimating the overall mean, $\sigma_{\hat{I}}$, from ordinary MCS (based on Eqs. (7)–(9)) and from proportionate stratified sampling (based on Eqs. (12)–(14)). The horizontal axis is the total number of samples, N, which for proportionate sampling equals the number of strata ($K = 16$) times the number of samples per stratum N_k, the latter being varied from 1 to 1024 in powers of 2 (that is, the total number of samples varies from 16 to 16 384). For ordinary MCS, the errors are much larger when there is substantial variability between the classes. For proportionate stratified sampling, however, since each stratum is sampled the same number of times, the variations of the means between the strata are always perfectly sampled. Hence the rms error is the same for all cases considered; specifically, it always goes as $1/\sqrt{N}$. When variations within the strata are dominant (the weak variations case), MCS and stratified sampling lead to essentially the same errors.

3. APPLICATION TO OUTDOOR SOUND PROPAGATION

3.1 Refraction Categories Based on MOST

As mentioned in the Introduction, refractive conditions for outdoor sound propagation are often partitioned into strata. Such schemes have typically been based on Pasquill classes [2] or the Monin-Obukhov similarity theory (MOST). In this section, we provide a brief overview of MOST and systematically derive appropriate strata for sound refraction. Then, we use these strata for an illustrative calculation of variance reduction.

MOST is widely used to describe turbulence statistics in the atmospheric surface layer (ASL, roughly the lowermost 50–200 m of the atmosphere), including the mean vertical profiles of wind, temperature, and humidity. Ref. [6] considers in detail the systematic application of MOST to refraction of sound rays. For simplicity, we assume that the rays are oriented within about 20° of horizontal, and thus refraction may be modeled on the basis of vertical gradients of the effective sound speed, which is defined as $c_{\text{eff}}(z,\psi) = c(z) + v_\perp(z)\cos\psi$, where $c(z)$ is the actual sound speed, $v_\perp(z)$ the horizontal component of wind, ψ the azimuthal angle between the wind and propagation directions, and z the height. A negative vertical gradient in c_{eff} causes upward refraction (away from the ground), whereas a positive gradient causes downward refraction (toward the ground). MOST predicts the following equation for the gradient [6]:

$$\frac{\partial c_{\text{eff}}}{\partial z} = \frac{1}{k_v z}\left[P_t c_* \phi_h(\xi) + u_* \cos(\psi)\,\phi_m(\xi)\right] - \frac{g(\gamma-1)}{2c_0}. \tag{17}$$

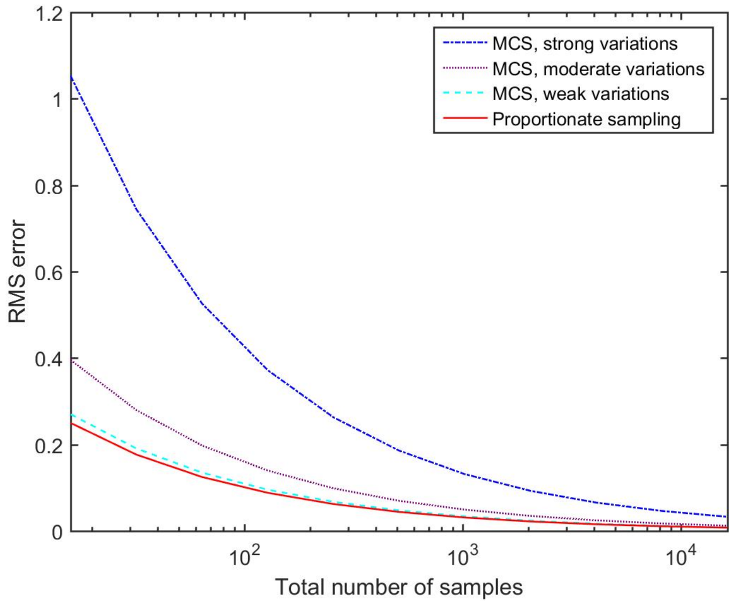

Figure 3: Errors for predicting the overall mean for the three cases shown in Fig. 2, as a function of the total number of samples, N. Shown are curves for ordinary Monte Carlo sampling (MCS) and for proportionate stratified sampling. For the latter, all cases reduce to the same curve.

Here, u_* is the friction velocity, $c_* = (c_0/2T_0)\, T_*$ is a characteristic scale of the sound-speed fluctuations, c_0 and T_0 are reference values of the sound speed and temperature, g is gravitational acceleration, $k_v \simeq 0.40$ is von Kármán's constant, $P_t \simeq 0.95$ is the turbulent Prandtl number in neutral stratification, γ is the ratio of specific heats for air, $T_* = -Q_H/\left(\rho_0 c_P u_*\right)$ is the surface-layer temperature scale, Q_H is the sensible heat flux from the surface to the overlying air, ρ_0 is the air density, and c_P is the specific heat at constant pressure. Furthermore, $\phi_h(\xi)$ and $\phi_m(\xi)$ are universal functions of the non-dimensional height $\xi = z/L_o$, where $L_o = -u_*^3 T_0 \rho_0 c_P/\left(g k_v Q_H\right)$ is the *Obukhov length*. Many forms for $\phi_h(\xi)$ and $\phi_m(\xi)$ have been proposed in the literature; the ones used for the calculations in this paper are given in Ref. [6].

The first term on the right-hand side of Eq. (17) is the contribution from temperature gradients. It can be positive or negative, depending on the sign of c_* (which is determined by stability in the atmosphere). The second term is the contribution from wind gradients. This term can also be positive or negative, depending on the sign of $\cos\psi$. The third term is due to adiabatic compression of the air column. The first and second terms on the right, when integrated, have an approximately logarithmic behavior; they change rapidly near the ground and become weaker as z increases. The adiabatic term, on the other hand, is independent of height. Although it produces a relatively small gradient, it becomes dominant for large z.

A useful simplification of Eq. (17) involves generalizing the definition of the turbulent Prandtl number to include dependence on the non-dimensional height ξ, specifically $P_{t,h}(\xi) \equiv P_t \phi_h(\xi)/\phi_m(\xi)$. We furthermore approximate $P_{t,h}(\xi)$ with P_t, which results in

$$\frac{\partial c_{\text{eff}}}{\partial z} \simeq \frac{P_t c_{\text{eff}}^*}{k_v z} \phi_m\left(\xi\right) - \frac{g\left(\gamma - 1\right)}{2c_0}, \tag{18}$$

where

$$c_{\text{eff}}^* \equiv c_* + (u_*/P_t)\cos\psi = (u_*/P_t)(A + \cos\psi) \tag{19}$$

and $A = P_t c_*/u_*$ is a dimensionless parameter indicating the importance of the sound-speed fluctuations relative to the wind-velocity fluctuations.

The case $|A| \ll 1$ corresponds to nearly neutral atmospheric stratification. In such conditions, which are typical of a windy day or night with cloud cover, wind gradients dominate. The case $A \ll -1$ corresponds to unstable atmospheric stratification, as typically occurs on a sunny afternoon with light wind, for which the

Table 1: Ranges for "refraction strength" categories based on the effective sound-speed scale, c^*_{eff}.

Range	Description
$c^*_{\text{eff}} < -0.5\,\text{m/s}$	very strong upward refraction
$-0.5\,\text{m/s} < c^*_{\text{eff}} < -0.3\,\text{m/s}$	strong upward refraction
$-0.3\,\text{m/s} < c^*_{\text{eff}} < -0.1\,\text{m/s}$	moderate upward refraction
$-0.1\,\text{m/s} < c^*_{\text{eff}} < 0.1\,\text{m/s}$	weak refraction
$0.1\,\text{m/s} < c^*_{\text{eff}} < 0.3\,\text{m/s}$	moderate downward refraction
$0.3\,\text{m/s} < c^*_{\text{eff}} < 0.5\,\text{m/s}$	strong downward refraction
$0.5\,\text{m/s} < c^*_{\text{eff}}$	very strong downward refraction

Table 2: Ranges for "profile shape" categories based on the inverse Obukhov length, L_o^{-1}.

Range	Description
$-0.5\,\text{m}^{-1} < L_o^{-1} < -0.1\,\text{m}^{-1}$	strongly convective
$-0.1\,\text{m}^{-1} < L_o^{-1} < -0.02\,\text{m}^{-1}$	moderately convective
$-0.02\,\text{m}^{-1} < L_o^{-1} < -0.005\,\text{m}^{-1}$	weakly convective
$-0.005\,\text{m}^{-1} < L_o^{-1} < 0.005\,\text{m}^{-1}$	neutral
$0.005\,\text{m}^{-1} < L_o^{-1} < 0.02\,\text{m}^{-1}$	weakly stable
$0.02\,\text{m}^{-1} < L_o^{-1} < 0.1\,\text{m}^{-1}$	moderately stable

effective sound speed gradient is dominated by the temperature gradient and always negative. Finally, when $A \gg 1$, stratification is stable, as typically occurs on a clear night with calm wind. Near the ground, the gradient is positive for all propagation directions.

From Eq. (18), refraction categories can be formulated on the basis of c^*_{eff} and L_o, as these are the only two parameters that vary with weather conditions and propagation direction. In reference [15], a scheme based on seven categories for c^*_{eff}, and six for L_o^{-1}, was proposed. These categories are associated with the strength of the gradient and the shape of the profile, respectively. The suggested ranges are shown in Tables 1 and 2. Of course, fewer or more categories could be employed, depending on the desired fidelity.

3.2 Acoustical Example

To illustrate how this analytical framework applies to sound propagation predictions, we consider here a purely contrived dataset, but which is hopefully nonetheless informative. The data, shown in Fig. 4, are intended to mimic A-weighted sound levels after the source signal has propagated over a distance of O(1 km), so that meteorological effects are significant. The 7×6 matrix in the figure corresponds to all combinations of the refractive strength and profile shape cases from Tables 1 and 2. Each entry has three rows. The top row is the probability (in percent) for that strength/shape category (stratum). The middle row is the sound level prediction for the stratum, $\langle \hat{I}_k \rangle$, followed by the true value, $\hat{I}_k$, in parentheses. (Note that, in real-world situations, we do not have access to the true value.) The bottom row is the standard deviation of the sound level within that stratum, $\sigma_{\hat{I}_k}$.

To make the dataset somewhat more realistic, we have included a tendency to underpredict sound levels in upward-refracting conditions, as often happens due to underprediction of scattering by turbulence or diffraction. We also include a tendency for MOST to overpredict sound levels in stable atmospheric conditions; this occurs because the temperature inversion is modeled as extending indefinitely above the surface, whereas in the real atmosphere the inversion generally does not extend higher than tens of meters. Many other factors could also bias the predictions; for example, if the ground impedance is assumed to be known exactly, but the modeled impedance differs from the scenario for which the predictions are made, there will be a bias. The mean bias error for the entire dataset is -0.76 dB. Regarding the standard deviations of the sound levels, we use a large value for upward refracting conditions, due to the importance of random scattering in such

	strongly convective	mod. convective	weakly convective	neutral	weakly stable	mod. stable
very strong upward	3% 52 dB (56 dB) 12 dB	2.5% 51 dB (55 dB) 12 dB	2.5% 50 dB (54 dB) 12 dB	2% 50 dB (54 dB) 12 dB	0% 52 dB (55 dB) 12 dB	0% 55 dB (57 dB) 12 dB
strong upward	5% 57 dB (61 dB) 12 dB	4% 56 dB (59 dB) 12 dB	3% 56 dB (59 dB) 12 dB	3% 56 dB (59 dB) 12 dB	1% 58 dB (60 dB) 12 dB	0% 59 dB (61 dB) 12 dB
moderate upward	3% 62 dB (64 dB) 10 dB	4% 61 dB (63 dB) 10 dB	4% 61 dB (63 dB) 10 dB	4% 61 dB (62 dB) 10 dB	2% 62 dB (63 dB) 10 dB	1% 63 dB (64 dB) 10 dB
weak refraction	1% 65 dB (65 dB) 8 dB	3% 65 dB (65 dB) 8 dB	4% 65 dB (65 dB) 8 dB	4% 65 dB (65 dB) 8 dB	4% 66 dB (66 dB) 8 dB	2% 67 dB (67 dB) 8 dB
moderate downward	0% 67 dB (67 dB) 10 dB	1.5% 67 dB (67 dB) 10 dB	3% 68 dB (68 dB) 10 dB	4% 69 dB (69 dB) 10 dB	5% 71 dB (71 dB) 10 dB	4% 72 dB (71 dB) 10 dB
strong downward	0% 69 dB (68 dB) 12 dB	0% 70 dB (69 dB) 12 dB	1.5% 70 dB (70 dB) 12 dB	3% 71 dB (71 dB) 12 dB	4% 73 dB (72 dB) 12 dB	5% 76 dB (73 dB) 16 dB
very strong downward	0% 70 dB (68 dB) 12 dB	0% 71 dB (70 dB) 12 dB	0% 71 dB (71 dB) 12 dB	2% 72 dB (72 dB) 12 dB	2% 75 dB (73 dB) 16 dB	3% 80 dB (74 dB) 20 dB

Figure 4: Illustrative problem with refractive strength and shape categories (strata). The top row in each box is the probability of that stratum occurring. Middle row is predicted sound level for the stratum, followed by the actual value in parentheses. Bottom row is the standard deviation of the sound level within that stratum.

conditions. We also use a large value for strong downward refraction, due to the prevalence of ducted sound propagation, which results in a modal interference pattern that is challenging to predict accurately [16]. Other possible sources of variability include randomly varying wind direction and ground properties.

Calculations of the rms error for predicting the mean sound level, $\sigma_{\hat{I}}$, based on Eqs. (12)–(14), are shown in Fig. 5. Curves for equal and proportionate sampling are shown. By equal sampling, we mean that the same number of samples are taken from each stratum, regardless of its probability. Calculations are shown for one sample per stratum (a total of 42 samples), 2 samples per stratum (84 samples), and so forth in powers of 2 up to 256 samples per stratum. In proportionate sampling, as described in Sec. 2.3, the number of samples is apportioned according to the probability of occurrence for the stratum. In either case, the general trend is for the rms error to decrease as the total number of samples increases, as would be expected. The curves plateau to a fixed value, which corresponds to the average bias error. Perhaps surprisingly, the rms error is only slightly reduced through proportionate sampling.

4. CONCLUSION

The practice of partitioning meteorological and refractive conditions into classes (or *strata*, in statistical terminology) has a long history in outdoor sound propagation. There are various motivations for adopting such classes; typically they are used as part of a process for improving the computational efficiency of propagation predictions. However, the statistical benefits are rarely considered from a fundamental or quantitative perspective. The discussion and examples in this paper were intended to illuminate some of the pertinent statistical sampling issues. In future work, we intend to apply these concepts to the analysis of a large synthetic database of excess attenuation calculations, as generated by the parabolic equation method and spanning a large range of ground, refractive, and turbulence conditions. Such an analysis will hopefully provide insight on the best schemes for formulating the strata, and for quantifying the variance reductions.

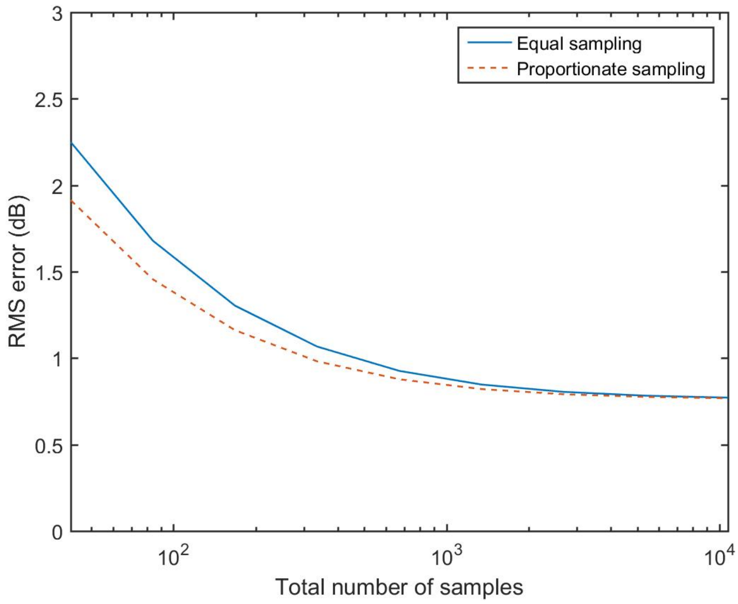

Figure 5: Dependence of the RMS error for estimating mean sound level on the number of sample predictions. Two curves are shown, one when the number of samples in the strata are equal, and the other when the strata are sampled in proportion to their probability of occurrence. The axis shows the total number of samples.

ACKNOWLEDGEMENTS

This research was funded by the U.S. Army Engineer Research and Development Center (ERDC). Any opinions expressed in this paper are those of the authors and not the ERDC or U.S. Army. Permission to publish was granted by Director, Cold Regions Research and Engineering Laboratory.

REFERENCES

[1] K. J. Marsh. The CONCAWE model for calculating the propagation of noise from open-air industrial plants. *Appl. Acoust.*, 15(6):411–428, 1982.

[2] F. Pasquill. The estimation of the dispersion of windborne material. *Meteorol. Mag.*, 90(1063):33–49, 1961.

[3] V. Zouboff, Y. Brunet, M. Berengier, and E. Sechet. A qualitative approach of atmospherical effects on long range sound propagation. In *Sixth International Symposium on Long-Range Sound Propagation*, pages 251–269, 1994.

[4] R. Raspet and R. K. Wolf. Application of the fast field program to the prediction of average noise levels around sources. *Appl. Acoust.*, 27(3):217–226, 1989.

[5] D. Heimann and E. M. Salomons. Testing meteorological classifications for the prediction of long-term average sound levels. *Appl. Acoust.*, 65(10):925–950, 2004.

[6] V. E. Ostashev and D. K. Wilson. *Acoustics in Moving Inhomogeneous Media*. CRC Press, Boca Raton, FL, second edition, 2015.

[7] J. S. Bendat and A. G. Piersol. *Random Data: Analysis and Measurement Procedures*. Wiley, New York, 2011.

[8] D. S. Wilks. *Statistical Methods in the Atmospheric Sciences*. Elsevier, Oxford, third edition, 2006.

[9] M. Evans and T. Swartz. *Approximating Integrals Via Monte Carlo and Deterministic Methods*. Oxford University Press, Oxford, 2000.

[10] D. P. O'Leary. Multidimensional integration: partition and conquer. *Comput. Sci. Eng*, Nov-Dec:58–66, 2004.

[11] W. L. Dunn and J. K. Shultis. *Exploring Monte Carlo Methods*. Elsevier, Amsterdam, 2011.

[12] P. Chevret, P. Blanc-Benon, and D. Juvé. A numerical model for sound propagation through a turbulent atmosphere near the ground. *J. Acoust. Soc. Am.*, 100(6):3587–3599, 1996.

[13] K. E. Gilbert, R. Raspet, and X. Di. Calculation of turbulence effects in an upward-refracting atmosphere. *J. Acoust. Soc. Am.*, 87:2428–2437, 1990.

[14] J. C. Helton, J. D. Johnson, C. J. Sallaberry, and C. B. Storlie. Survey of sampling-based methods for uncertainty and sensitivity analysis. *Reliab. Eng. Syst. Safe.*, 91:1175–1209, 2006.

[15] D. K. Wilson, V. E. Ostashev, and M. Mungiole. Categorization schemes for near-ground sound propagation. In *18th International Congress on Acoustics*, 2004.

[16] D K. Wilson, M. S. Lewis, J. W. Weatherly, and E. L Andreas. Dependence of predictive skill for outdoor narrowband and broadband sound levels on the atmospheric representation. *Noise Control Eng. J.*, 56(6):465–477, 2008.